

# Diffuse Optical Tomography with an amplified ultrafast laser and a single-shot streak camera : application to real time *in vivo* songbird neuro-imaging.

Hugues Guillet de Chatellus <sup>a</sup>, Clémentine Vignal <sup>a,b</sup>, Stéphane Ramstein <sup>a</sup>, Nicolas Verjat <sup>a</sup>, Nicolas Mathevon <sup>b</sup>, Stéphane Mottin <sup>a \*</sup>

<sup>a</sup> LTSI, Université Jean Monnet, UMR 5516, 10 rue Barrouin, 42000 Saint-Etienne

<sup>b</sup> ENES, Université Jean Monnet, 42 rue Paul Michelon, 42023 Saint-Etienne

\* [mottin@univ-st-etienne.fr](mailto:mottin@univ-st-etienne.fr)

Mottin, S. identifier: <http://orcid.org/0000-0002-7088-4353>

## Reference BibTeX:

```
@article{2005_mottin_25,  
  TITLE = {Diffuse optical tomography with an amplified ultrafast laser and a single shot streak camera:  
  application to real-time in vivo songbird neuroimaging},  
  AUTHOR = { Guillet De Chatellus, Hugues and Vignal, Clémentine and Ramstein, Stéphane and Verjat,  
  Nicolas and Mathevon, Nicolas and Mottin, Stéphane },  
  JOURNAL = {SPIE},  
  VOLUME = { 5964},  
  PAGES = { 1-8},  
  YEAR = {2005},  
  DOI = {10.1117/12.624775},  
  KEYWORDS = {Diffuse Optical Tomography;time-resolved near-infrared spectroscopy;neuro-  
  imaging;brain energy metabolism;bird},  
}
```

---

## ABSTRACT

A new ultrafast Diffuse Optical Tomography (DOT) has been developed for real time *in vivo* brain metabolism monitoring in songbird. The technique is based on space resolved time of flight measurements of the photons across the brain tissues. A three dimensional reconstruction of the brain activity is foreseeable by means of a double space and time sampling of the reflectance signal. The setup and the treatment procedure are described in depth and promising preliminary results showing the response of brain tissues to hypercapnia stimulations (increase of CO<sub>2</sub>) are presented.

**Keywords :** Diffuse Optical Tomography, time-resolved near-infrared spectroscopy, neuro-imaging, brain energy metabolism

## INTRODUCTION

Among the different optical methods developed to probe cerebral tissues, ultrafast Diffuse Optical Tomography (DOT) has been proven to be a promising technique and presents potential advantages over other techniques (MRI, electrophysiology). It is non-invasive, non-irradiant and can be performed *in vivo* and potentially, in freely moving configuration. It is based on the measurement of the optical parameters of a tissue, especially the absorption coefficient in the near infrared [1-3]. According to data in the vertebrates, HbO<sub>2</sub> and Hb present a large difference of absorption, the

maximum of this difference being localized around 650-700 nm. Light absorption measurements are thus quantitatively related to tissues oxygenation [4,5] and are consequently good indexes of cells activity [6]. However, in spite of many academic and industrial developments, DOT in the continuous wave (CW) regime has never been granted a clinical validation, due to the entanglement of many different parameters (both physical and structural) contributing to the detected signal. On the contrary, ultrafast (*i.e.* fs) DOT has been proven to be a reliable tool for characterizing the optical properties of diffusive media like brain tissues: contrary to CW DOT where a single parameter is measured (*i.e.* the transmission), ultrafast DOT enables to access a whole distribution of photons times of flight, giving much more information on the optical and structure properties of the medium [7, 8]. In particular in-depth scanning is foreseeable since each time of flight corresponds to a particular exploration volume (see Fig. 1). It is therefore promising to combine ultrafast DOT with transverse imaging properties to get a full mapping of the probed brain tissues. Solutions based on multiple source and detection fibres have been proposed in the frame of CW DOT with the constraint imposed by the necessity of positioning multiple fibres on the surface of the skull. Here we chose to implement ultrafast DOT in an imaging configuration that enables to collect the photons emerging from a whole segment apart from a single source fibre. The x resolution is given by these imaging properties ; the z resolution could be estimated by the shape of the time of flight distribution. The use of a fs broadband white laser could also enables a  $\lambda$  resolution [8]. Only single wavelength procedures are described in this paper.

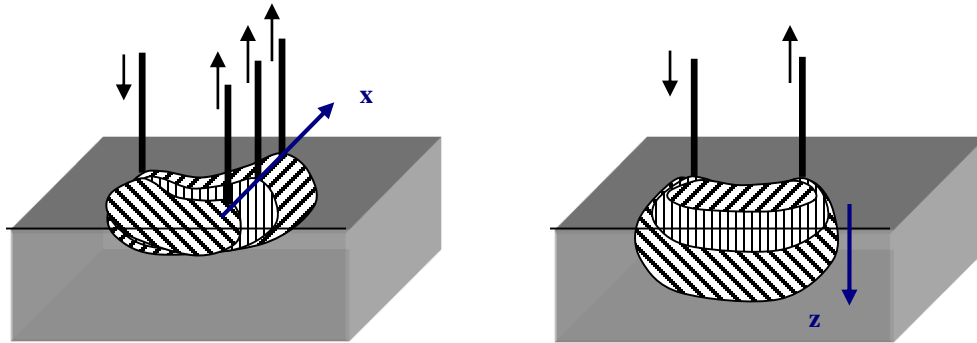


Fig. 1. Left : variation of the volume explored by the photons with respect to the position of the collection point, for a given delay after the light pulse. Right : variation of this volume for different time delays after the light pulse, for a given collection point.

Ultrafast DOT can apply to a great variety of subjects in biology, from small animals to humans, to probe the brain activation. We chose to test it in the general context of the cognitive capabilities of birds, the goal being the imaging of specific brain areas involved in song processing in songbird : the *Caudal Nidopallium* (NCM). We report here the first approach for mapping the functional neuro-energetics in songbird with simultaneous 1D imaging and ps resolution of the photons times of flight, allowing the best resolution of single-shot DOT techniques.

## ULTRAFAST DOT FOR SONGBIRD NEURO-IMAGING

### 1. General description of the setup

The experimental setup combines an ultrafast broadband laser source delivered on the surface of the bird, an imaging system to collect the photons diffused through the brain tissues and a single shot streak camera as a detection system.

#### 1.1. Laser source

The ultrafast laser source is a supercontinuum (450 nm to 950 nm) obtained by focusing amplified ultrafast laser pulses into pure water [9]. The pulses (170 fs, 0.5 mJ, 1 kHz) are produced by a Ti:Sa chirped-pulse amplification laser chain

(Coherent Vitesse XT and BMI/Thales alpha 1000). This configuration presents two main advantages. First, reflectance experiments can be carried out at different wavelengths simply by inserting a narrow bandwidth optical filter on the path of the continuum. Second, it enables spectrum-resolved experiment in conjunction with a spectrometer in front of the detection system. The generated white light continuum is coupled into an optical fibre (core diameter 200  $\mu\text{m}$ , numerical aperture 0.4, length 30 cm). The average power is lowered below 2 mW, in order to avoid optical damage of the brain tissues. The fibre is placed at the surface of the skull of the bird (see below).

## 1.2. Imaging system

An imaging setup based on two lenses (L4, L1, see Fig. 2) (100 mm focal length) conjugates optically the surface of the skull with the plane of the entrance slit of the streak camera. An afocal system made of two lenses (L2, L3) (100 mm focal) is placed between the two imaging lenses, and a slit (F) is put at the focal point of the afocal system. This slit is optically conjugated with the entrance slit of the streak camera (length 5 mm, width 70  $\mu\text{m}$ ), resulting in a great simplification of the alignment procedure and in the possibility of controlling the intensity of the light by narrowing the slit as well. The magnification of the set-up is 1. Intrinsic filtering properties of the imaging setup enable to collect only the photons emerging from a 5 mm-long segment located 5 mm apart from the fibre, so as to probe auditory regions of the NCM (Fig. 5). The position of this segment on the head of the bird can be controlled by eye by shining the intermediate slit with a He-Ne laser and checking and adjusting the position of its image on the skull (mirror M). We put a narrow bandwidth filter (IF) (10 nm FWHM) centred at 700 nm, where the difference of absorption between the two haemoglobin species is maximal.

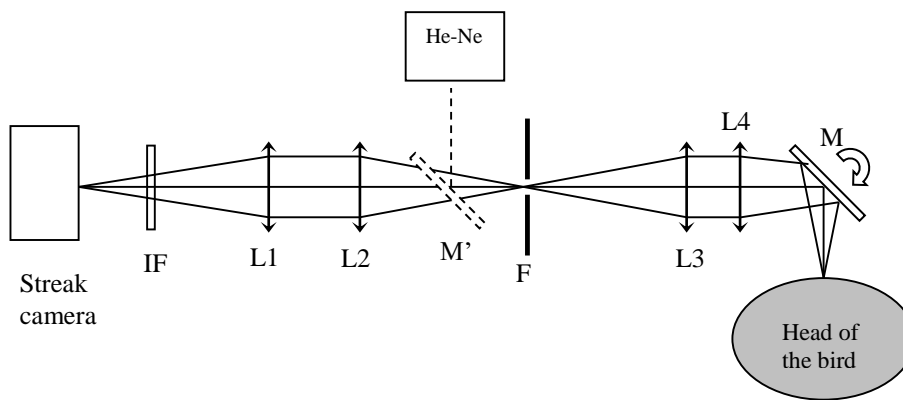


Fig. 2. Sketch of the imaging set-up

## 1.3. Detection system

The imaging system conjugates a segment of the head of the bird with the entrance slit of the single shot streak camera (Hamamatsu Streakscope C4334), that measures the propagation time of the photons through tissues with a temporal resolution of 20 ps (see further). With a deconvolution procedure a temporal resolution below 8 ps could be achieved. The Charged Coupled Device (CCD) display is made of 640 (x)\*480(time) pixels. All measurements are carefully corrected from the shading effects. Each measurement consists in a frame integrating 33 laser pulses due to the 33 ms CCD integration time of the streak camera. The sweep of the streak camera is triggered by a fast photodiode measuring a leaking in the optical amplifier. An electric delay line compensates for the electronic delay of the streak camera controller. The time base is set to 1 ns and images are stored at the video rate (30 images/s) on a computer. Recall that the length of the entrance slit of the camera (5 mm) corresponds to 640 pixels.

## Imaging properties

The numerical aperture of the setup is 0.1 with a magnification of 1 (within 10%). The magnification was determined by imaging a ruler. The spatial resolution (i.e. along the slit) was also determined by imaging a white sheet of paper half covered with black ink. The image consists in the response of the system to a Heaviside step and characterizes the spatial resolution of the set-up (optical set-up + streak camera). From Fig. 3, it is found to be close to 600  $\mu\text{m}$ .

The temporal resolution of the system is set by the temporal width of the trace on the CCD camera of an ultrashort pulse. By sending directly a leaking of a sub-picosecond laser pulse, we get the instrument response function. By averaging  $10^5$  laser shots, we obtain a 10 pixels-wide temporal trace (FWHM) corresponding to approximately 20 ps.

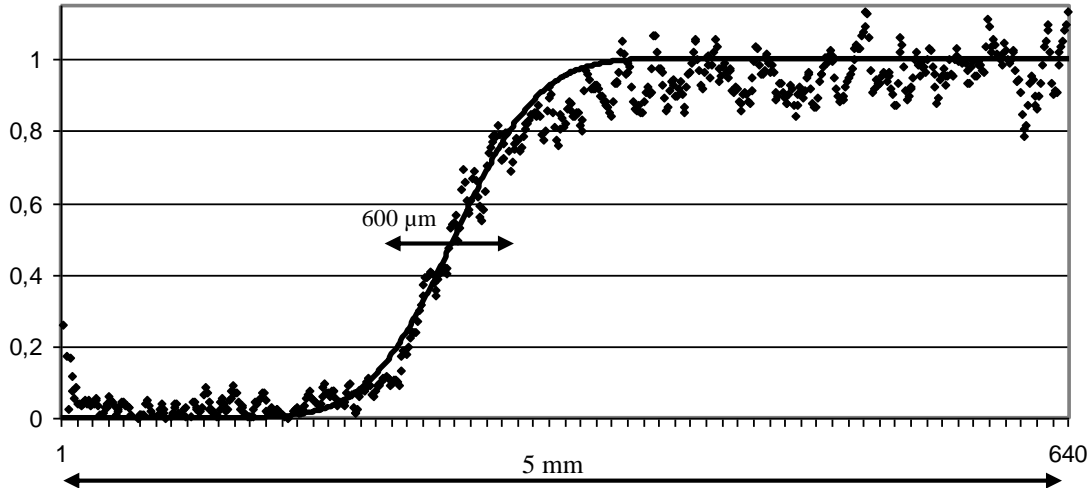


Fig. 3. Intensity measured by the streak camera when imaging a half black screen (see text). The solid curve is a fit by the function *erf*.

## 2. Data processing

In this paragraph we present the technique we developed to extract information from the streak images both in terms of spatial (along  $x$ ) and temporal (along  $z$ ) resolutions.

Compared to DOT with “discrete” detectors, ultrafast DOT in an imaging configuration allows to characterize the space and time differential operators ( $\partial/\partial x$ ,  $\partial/\partial t$ ,  $\partial^2/\partial x \partial t$ ). As a first attempt, each streak camera image (30 Hz) (dimensions 640\*480 pixels) is divided into 8 space areas and processed analytically. The reason why we divide the image in 8 parts is to limit the total volume of information and to get a good dynamics in terms of signal to noise ratio. Physically, each one of these 8 areas corresponds to a 600  $\mu\text{m}$  –long dash on the segment imaged by the system. We define a set of parameters that characterize the shape of the reflectance curve in all the 8 space areas. Any change in these values is a signature of a change of the optical properties in the volume explored by the photons between the fiber and the dash corresponding to the considered space area. The reflectance curve is divided in five temporal zones. The first one contains all the photons detected from  $t = 0$  to the time  $t_{20\%}$  where 20 % of the photons have arrived. The proportion of photons in the area is therefore  $p_0 = 20\%$ . Three 30 pixels (62 ps)-wide other areas are defined from the position of  $t_{20\%}$  and located respectively 62 ps, 124 ps and 186 ps after  $t_{20\%}$  (see Fig. 4 and Fig. 5). The last one contains all the photons arriving after  $t_{20\%} + 248$  ps. Note that the  $p_i$  parameters characterize relative variations of the shape of the reflectance curve since the values are normalized with respect to the total integrated area of the curve ( $\sum p_i = 1$ ). We decided to normalize the parameters since an analysis based on the monitoring of the amplitude of the signal showed a signal to noise ratio significantly poorer than in the case of normalized data.

For each of these 8 space areas, the integration of the grey level values is carried out over all the pixels of the area and enables to determine the position of  $t_{20\%}$ . Then the space areas are divided in time zones and the proportion of photons detected in each space-time area is carried out. We obtain for the 8 space zones of a single image, a set of 4 parameters,  $p_1$ ,  $p_2$ ,  $p_3$ ,  $p_4$ . These parameters are averaged over 30 images to get a set of values per second and per space zone.

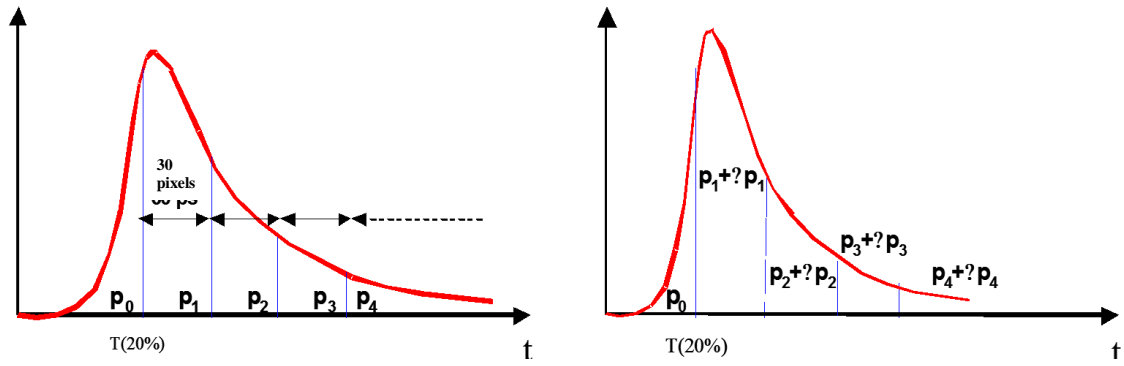


Fig. 4. Principle of the temporal sampling of the time of flight distribution curve.

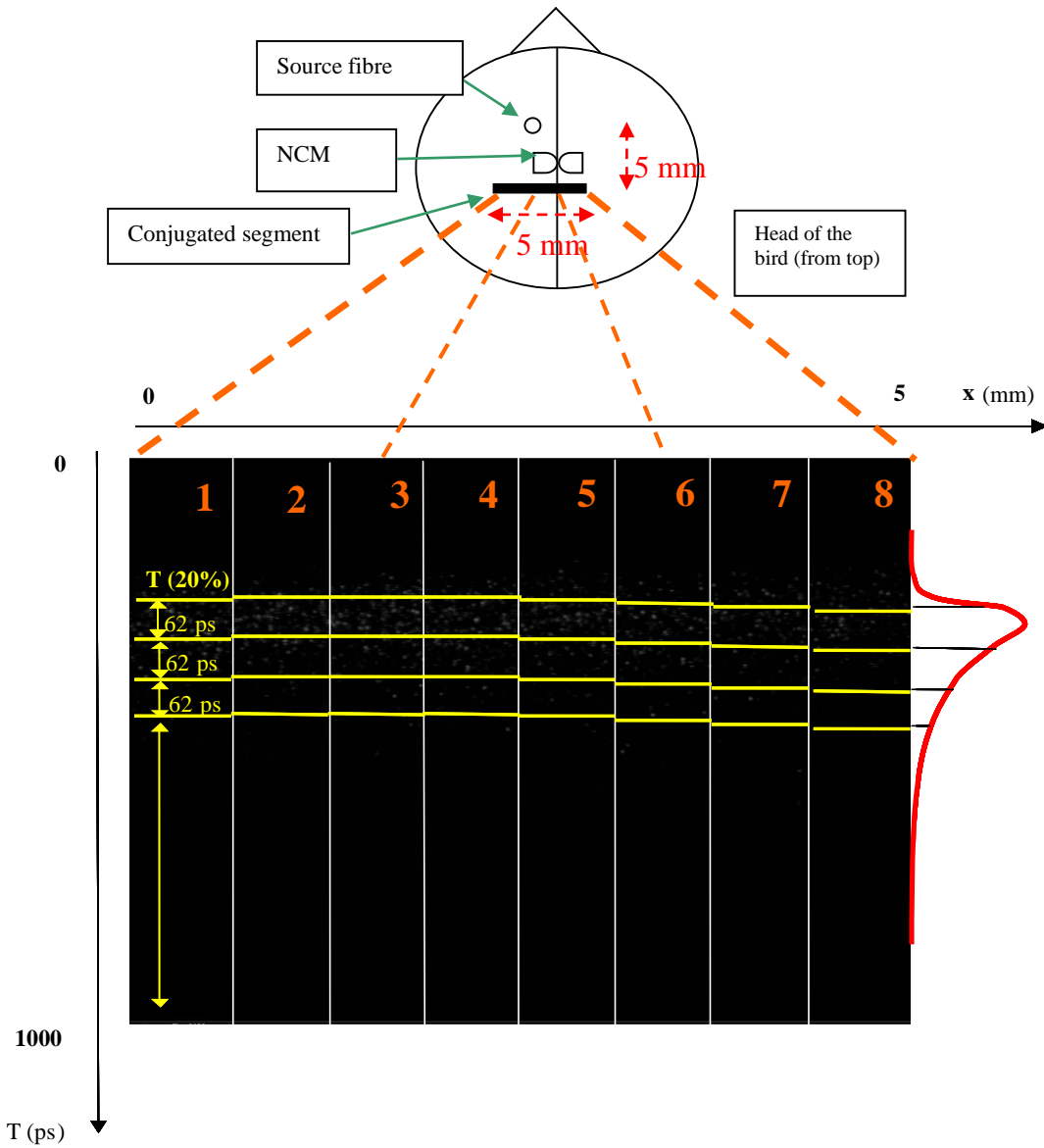


Fig. 5. Relationship between the geometry of the experiment and the space and time sampling of the single shot streak camera image. For practical reasons, the right and left of the bird's head are inverted.

### 3. Experiment

As a preliminary test before probing the response of the brain metabolism to song stimulations, we characterized the possibilities of our technique by means of normoxic hypercapnia stimulations, where the metabolism of the animal is artificially modified by the increase of carbon dioxide in the air breathed by the bird.

#### 3.1. Preparation and protocol

##### 3.1.1. Preparation of the bird (stereotaxy)

Three adult male zebra finches *Taeniopygia guttata* (20g body weight) were used as subjects for the experiments. These birds were bred in our aviary (Jean Monnet University, France) with 12L/12D photoperiod with adapted wavelengths, food and water *ad libitum*, temperature between 23°C and 25°C.

The zebra finches are anaesthetized with 1,8% isoflurane under spontaneous breathing. The anaesthetized birds with the head previously plucked (two days before experiments) are fixed in a stereotaxic frame (Stoelting Co., USA, adaptations for birds). For head transillumination, the optical fibre is fixed into stereotaxic manipulators (Stoelting Co., USA) and placed on the skin of the animal. The position of the input fibre is chosen in the right hemisphere. In order to probe the *caudal nidopallium* [9], the coordinates in millimeters is F1 (2.0, 5.4, -2.7) according to the origin point (0, 0, 0) defined by the intersection of the vertical plane passing through the interaural line and the sagittal suture (the *vena cerebrialis dorsocaudalis*). To insulate the bird from the background noise the stereotaxic setup containing the bird is placed in a sound-attenuating box (50 x 65 x 40 cm, depth x width x height). The bird inside the box is in contact with the manipulators only through the optical fibre and a little speaker placed inside the box for playback experiments and connected to a computer.

All birds had free access to food and water prior to anaesthesia. The experimental protocols were approved by the Jean Monnet University's animal care committee.

##### 3.1.2. Experimental protocol

After a 5 minutes baseline period of normocapnia, the gas content is varied and the proportion of CO<sub>2</sub> is set to 7% (O<sub>2</sub> : 20%, N<sub>2</sub> : 73%). The gas flow sent to the mask and the proportions of oxygen and isoflurane are not changed. After 5 minutes of hypercapnia, the gas content turns back to its normal values. After 10 minutes of normocapnia, a second 5 minutes long hypercapnia phase follows, before turning back to the normocapnia regime. Meanwhile the streak camera data is recorded. Data processing reveals the dynamics of the hypercapnia process with a sub-second resolution.

#### 3.2. Hypercapnia results

The average variation ( $\delta p_i$ ) of the parameters between normocapnia and hypercapnia is carried out over the three birds. The results are presented on Fig. 6. Experimental data show a relative decrease of short-time photons ( $p_1$ ) and a relative increase of long times photons. This corresponds qualitatively to a relative broadening of the time of flight distribution, associated with a fall of the absorption coefficient (at 700 nm). The effect is homogeneous in the 8 space areas. This result corresponds to a global increase of HbO<sub>2</sub> compared to Hb and confirms the usual effects of hypercapnia.

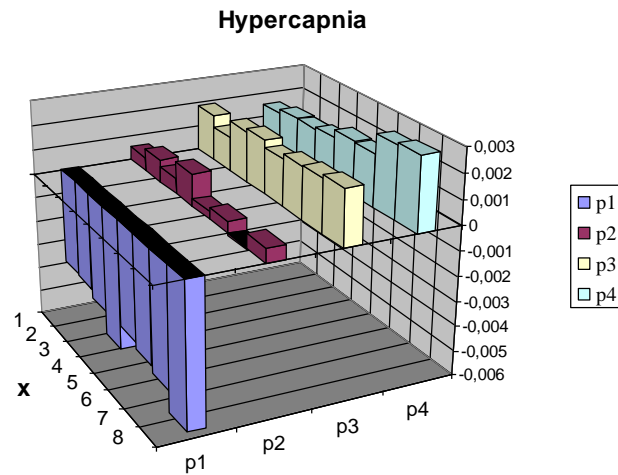


Fig. 6. Variation of the  $p_i$  parameters between the normocapnia and hypercapnia phases for the 8 space areas (average over 3 birds).

### 3.3. Future improvements and prospects

#### 3.3.1. Local brain stimulations

The ability of the technique as a true imaging method is about to be demonstrated. The experiment relies on the selective activation of specific auditory brain areas (NCM) by acoustic stimulations and the space-dependent probing of the reflectance signal. Experiments are in progress. Finite elements simulations (Femlab 3.1, comsol) have been performed on a three-dimensional model of songbird's head. Fig. 7 shows the theoretical variation of the  $p_i$  parameters when the single NCM is activated (increase of the absorption coefficient of 0.5 %). These simulations present a spatial contrast in the 8 probed space areas and show that the technique is able to localize (at least along x) the activated structures and is a promising candidate as a three-dimensional neuro-imaging method.

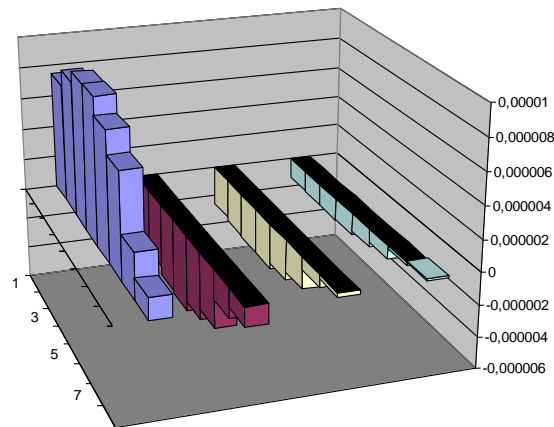


Fig. 7. Theoretical variation of the  $p_i$  parameters induced by stimulation of the NCM structure for all of the 8 space areas (finite elements methods).

### 3.3.2. Technical improvements

The versatility of the optical design we implemented has interesting advantages in terms of imaging. Simply by tilting the M mirror we can sweep the imaging segment and get the reflectance signal from a 2D area. This possibility is way more flexible than fiber bundles and leads to a narrower spatial resolution, not limited by the diameter of the optical fibers, but only by the numerical aperture and the properties of the optical setup. The tilt of the M mirror can be achieved by means of a fast piezo-electric transducer triggered by the optical amplifier.

Another interesting advantage comes from the possibility of contact-free measurements. Up to now the contact between the animal and the optical testing apparatus is only achieved by the source fibre. The imaging part is contact-free by definition. It would not be a big difficulty to make the apparatus completely contact-free simply by replacing the source fibre by an open-air beam controlled by lenses and mirrors. It is thus reasonable to imagine the extension of our design to a freely moving setup. This would avoid the difficulty raised by anaesthesia on the response of the brain to different stimulations and would be a decisive advantage over MRI techniques that require the constraints of stereotaxic conditions.

### ACKNOWLEDGEMENTS

These studies were supported by the Interdisciplinary Program “Cognition and Information Processing” (CTI 02-19) of the french Centre National de la Recherche Scientifique (CNRS) and by the Program “Emergence” of the Région Rhône-Alpes (H. G. de C.). C.V. is supported by the french Ministry of National Education. We thank Sabine Palle for her help during the NIRS experiments.

### REFERENCES

- [1] J. P. Culver, T. Durduran, D. Furuya, C. Cheung, J. H. Greenberg and G. Yodh, *J. Cereb. Blood Flow Metab.* **23**, 911-924 (2003).
- [2] N. Plesnila, C. Putz, M. Rinecker, J. Wiezorrek, L. Schleinkofer, A. E. Goetz and W. M. Kuebler, *J. Neurosci. Methods* **114**, 107-117 (2002).
- [3] “Optics in Neurosciences”, *J. Biomed. Opt.* (Jan/Feb 2005).
- [4] M. Cope, D. T. Delpy, E. O. Reynolds, S. Wray, J. Wyatt and P. van der Zee, *Adv. Exp. Med. Biol.* **222**, 183-9 (1988).
- [5] D. T. Delpy, M. Cope, P. Van der Zee, S. Arridge, S. Wray and J. Wyatt, *Phys. Med. Biol.* **33**, 1433-1442 (1988).
- [6] H. Obrig and A. Villringer, *J. Cereb. Blood Flow Metab.* **23**, 1-18 (2003).
- [7] S. Mottin, J-M. Tualle, “Introduction à la transillumination” in *Lasers et Technologies femtosecondes*, Ed. M. Sentis, O. Uteya, S. Mottin (PUSE, 2005), in press.
- [8] S. Ramstein, C. Vignal, N. Mathevon and S. Mottin, “In vivo and non-invasive measurement of songbird head’s optical properties” *Applied Optics*, in press (2005).
- [9] A. Brodeur and S. L. Chin, *J. Opt. Soc. Am. B* **16**, 637-650 (1999).